Preparation and properties of nanocomposite of poly(phenylene sulfide)/calcium carbonate

Xiaojun Wang[1], Wei Tong[1], Wei Li[1], Hengmei Huang[1], Jie Yang[2] (✉), Guangxian Li[1]

1. The College of Polymer Science & Engineering, Sichuan University; State Key Laboratory of Polymer Materials Engineering, Sichuan University, Chengdu, 610065, Sichuan, People's Republic of China
2. The Institute of Materials Science & Technology, Sichuan University, Chengdu, 610065, Sichuan, People's Republic of China
E-mail: ppsf@scu.edu.cn; Fax: +86-28-8541-2866

Summary

A way to prepare Poly (phenylene sulfide) (PPS) nanocomposite was introduced in the paper. The nanocomposite of PPS/$CaCO_3$ can be prepared by melt mixing process. The dispersion of the $CaCO_3$ nanoparticles in PPS was good when filler content below 5wt%. Differential scanning calorimeter (DSC) and small-angle light scattering (SALS) results indicated that the $CaCO_3$ nanoparticles could induce the nucleation but retard the mobility of polymer chains. The results of mechanical tests showed that a small amount of nanoparticles has resulted in a slight improvement in the tensile strength and a significantly 300% increase in the fracture toughness. We believe that the $CaCO_3$ nanoparticles can act as stress concentration sites, which can promote cavitation at the particles boundaries during loading. The cavitation can trigger mass plastic deformation of the matrix, leading to much improve fracture toughness.

Introduction

Poly (phenylene sulfide) (PPS) is an important high strength/high temperature engineering thermoplastic. PPS has a glass transition temperature of 85°C-90°C and melting temperature of about 290°C, and does not dissolve in any solvent below 200°C except strong acid. Even though PPS has these advantageous properties, it has weaknesses such as low impact strength and presents difficulties in injection molding. In order to overcome these problems, there have been studies on the crystallization and melting behaviors of PPS and its blends in the last decades [1-4]. The studies on the various PPS composites were also performed [5-8].

PPS is a kind of semicrystalline polymer. The mechanical and physical properties of the molded and extruded products of crystalline polymers are governed by the supermolecular morphology, which in turn is controlled by the crystallization process. The properties of semicrystalline polymer such as PPS depend on the crystallization behavior of the polymer. Thus, the study of the crystalline property is necessary for establishing the structure-property correlations in polymers.

Generally, in order to improve the impact and toughness of brittle polymers, it is common practice to add ductile polymers to the matrix. The problem is this method usually with the cost of the decreasing of the useful rigidity, measure-stability and heat-resistance at the same time of improving the toughness of matrix. During the last decades, making polymer/ nanoparticles composites has been an important path to tailor properties of polymeric materials because of their excellent properties and potential industrial applications [9-13]. The key is to control the dispersion of nanoparticles in polymer matrix. Layered silicates, such as montmorillonite, which has a fairly large aspect ratio as nanoparticles filler, have been extensively studied in recent years. Nanocomposites prepared with montmorillonite show improved strength, modulus, heat distortion temperature and barrier properties. In spite of many attractive improvement in physical and mechanical properties of the polymer/ (intercalated or exfoliated) clay nanocomposites, a significant drawback—low fracture toughness — has greatly limited their engineering applications. Other nanoparticles, such as silica and calcium carbonate ($CaCO_3$), have been used to prepare nanocomposites. Among them, $CaCO_3$ has been one of the most commonly used inorganic fillers for thermoplastics. And it has been reported that well dispersed $CaCO_3$ nanoparticles can significant improve the fracture toughness of the composites [14-15].

At present time, there are several published studies on PPS blends and composites, however, seldom studies are available on PPS modified by nanoparticles. Thus, in this investigation, composite of PPS/$CaCO_3$ nanoparticles was prepared in order to improve the impact properties, and its mechanical, thermal and crystalline properties were investigated. The toughening mechanisms involve during the fracture of the nanocomposites were proposed.

Experimental

Sample preparation

PPS pellets used in this investigation was a commercial grade resin (Haton, PPS-hb1, $M_n=3.2\times10^4$g mol^{-1}). The $CaCO_3$ nanoparticles were also a commercial grade obtained from Nano technology Inc. China (NPCC-200-SH, 40-60nm). Table 1 shows the compositions and sample code of PPS/$CaCO_3$ nanocomposites prepared in this investigation. Compounding was done using twin screw extruder with screws of 50 mm diameter. The barrel temperature was 290–320°C and screw speed was 140 rpm. The extrudate was pelletized, dried, and injection molded into standard test samples for mechanical properties test. The injection-molding temperature and pressure were 300°C and 70 MPa, respectively.

Table 1 compositions and sample code of PPS/ $CaCO_3$ nanocomposites used in this investigation

PPS/nano-$CaCO_3$ (wt.%)	100/0	98/2	97/3	95/5	90/10
Sample code	PPS0	PPS1	PPS2	PPS3	PPS4

Measurement and characterization

Tensile strength was measured by a Seiko test machine (AG-10TA) at room temperature and samples were measured according to standard GB/T-1040-1992. The

samples were in the form of dumb-bell with the gauge length of 50.0mm and cross-section of $10.0 \times 4.2 mm^2$(width×thickness). The data given are average of five measurements.

Unnotched impact strength was tested according to standard GB/T-1843-1996 by using Chengde Testing Machine (XJU-275). The dimensions of these samples were $100.0 \times 10.0 \times 4.2 mm^3$ (length×width×thickness). The data given are average of five measurements.

Morphologies of the fracture surface of the specimens were examined by a scanning electron microscope (SEM) (Hitachi S-450, Japan)with a accelerating potential 20KV after coated with gold in an automatic sputter coater. To investigate size and dispersion of nanoparticles, the freeze-fractured surface of the specimens were examined by scanning probe microscopy (SPM) (Seiko SPA-400, Japan) under a method of dynamic force microscopy (DFM).

Thermal analysis and crystallization properties of samples were carried out with differential scanning calorimeter (DSC) (EXSTAR6000 DSC6200) by Seiko with temperature calibrated with indium. All DSC measurements were performed under nitrogen atmosphere and samples were round sheet of about 10 mg. All samples were first heated to 320ºC at a heating rate of 20ºC/min, and then held at 320ºC for 10 mins to ensure an identical thermal history. The sample was subsequently cooled to room temperature at a cooling rate of 10ºC /min for data collection.

Crystallization properties were also obtained by small-angle light scattering (Home-made) method with H_V (cross polarized) scattering mode. The sample was melted at 320ºC and then isothermal crystallized at 160ºC in the setup to measure introduction time for crystallization.

Results and discussion

Dispersion of nanoparticles

The dispersion of a filler in the polymer matrix can have a significant effect on the mechanical properties of the composites. Therefore, it is very necessary to investigate the dispersion of a filler in the matrix of the composites. However, the dispersion of an inorganic filler in a thermoplastic is not an easy process. The problem is even more serious when using nanoparticles as a filler, because the nanoparticles have a strong tendency to agglomerate. Consequently, homogeneous dispersion of the nanoparticles in the thermoplastic matrix is, generally speaking, a difficult process. Fig. 1 shows the SPM photographs of PPS2, PPS3, and PPS4. The white plots in the SPM photographs represent the protuberances, namely the particles, on the freeze-fracture of the specimens. Therefore, the amount and the dispersion of particles in different composites can be observed. The patterns on the right side of SPM photographs in Fig.1 is the line profile of the profile line marked in the SPM photographs, and the data under each pattern is the dimensional information about the line profile. The 'Distance' is the width of two line cursors in the photograph, namely the diameter of the particles. SPM photographs show that the size of the nano-$CaCO_3$ particles is about 40-60nm, but the distance between nanoparticles decreases as the nano-$CaCO_3$ content increases, and especially at more than 5wt.% nano-$CaCO_3$ inclusion, the distance decreases more rapidly. Nano-$CaCO_3$ particles can be well distributed up to PPS3 which contain small amount of particle agglomerate, and congregated thereafter. Namely, the dispersion of nano-$CaCO_3$ in PPS matrix is significantly affected by
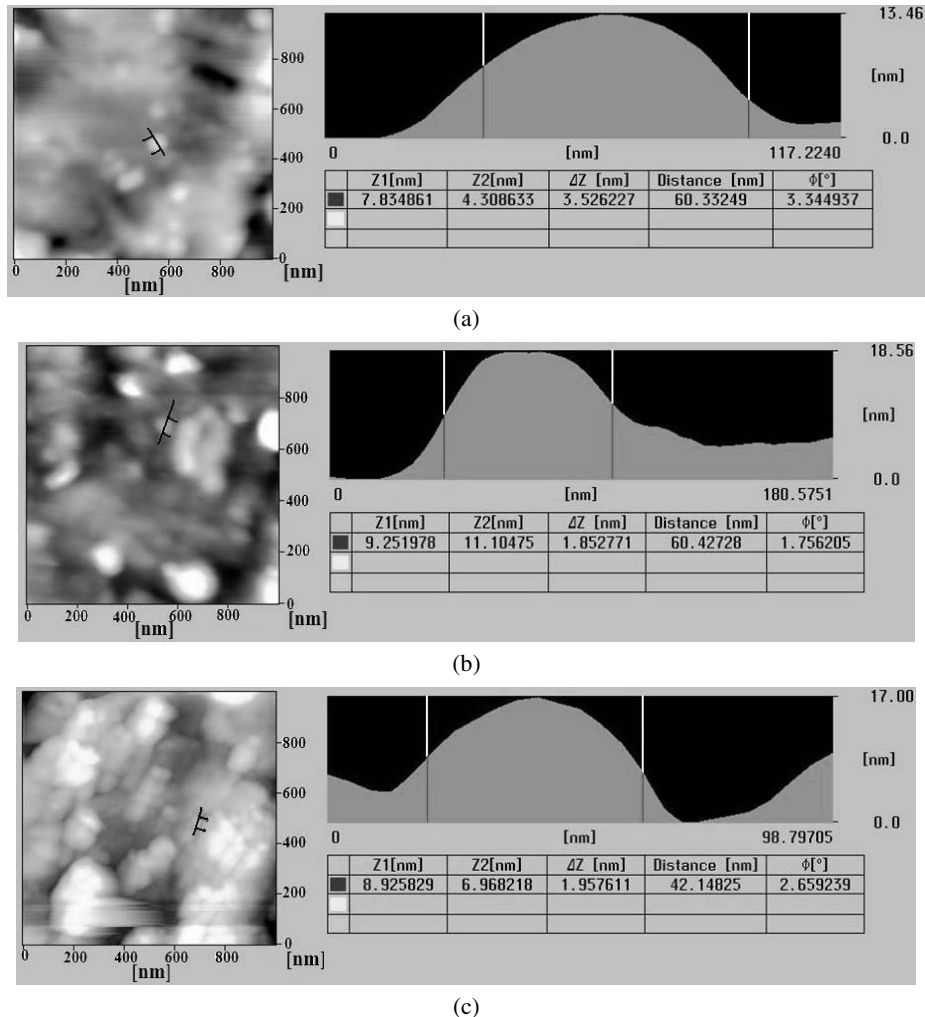
(a)

(b)

(c)

Fig.1 SPM figure of cross section of the nanocomposites. (a: PPS2; b: PPS3; c: PPS4.)

nano-CaCO$_3$ loading. This is reasonable considering that at high CaCO$_3$ concentrations, the interparticle distance is small, and hence agglomerate of these nanoparticles can occur during the melt mixing process and even after the mixing is stopped. Moreover, as the distance between the nano-CaCO$_3$ particles irregularly decreases, applied stresses can not be evenly distributed within the system and result in the stress concentration in a certain area. Whereas, PPS2 and PPS3 show a relatively even distribution of nano-CaCO$_3$ particles. From these SPM observations, nano-CaCO$_3$ particles in low loading systems (≤5wt.%) show a well dispersion.

Thermal and crystallization characteristics

It is known that the mechanical properties of the composites can be significantly changed if the crystallization characteristics of polymer matrix have been altered.

Fig.2 shows the DSC curves for the pure PPS and the nanocomposites. The DSC results indicate the crystallizing temperature of PPS is decreased by at most 5°C when a small amount of CaCO$_3$ ($\leq$5wt.%) is added to the PPS and thereafter the crystallizing temperature is increased. It is also obviously being found that the crystallinities of PPS are dramatically decreased with increasing the content of nanoparticles (Table 2). Rong et al. [16] found that the addition of nanoparticles of SiO$_2$ (particle size of 7nm) does not have any significant effect on the crystallinity and the crystallization temperature of matrix polymer. Another study [17] has shown that the addition of CaCO$_3$ (particle size of 40nm) increase of 10°C in the crystallization temperature of PP and suggest that the CaCO$_3$ nanoparticles are a very effective nucleating agent. However, in our case, the results show that a significant decrease of both crystallization temperature and crystallinity is achieved, imply that the presence of the CaCO$_3$ nanoparticles restrained the crystallization of PPS at a small loading and then hastened the crystallization with an increasing loading. In the light of foregoing discussion of the dispersion of nanoparticles, it is reasonable to propose that the well dispersed CaCO$_3$ nanoparticles may have great interfacial interaction with the polymer and prevent molecular chain to move and to line into lamella. While, with an increasing loading of CaCO$_3$, the nanoparticles can not be evenly distributed and form agglomerates which represent as nucleating agent during PPS crystallization.
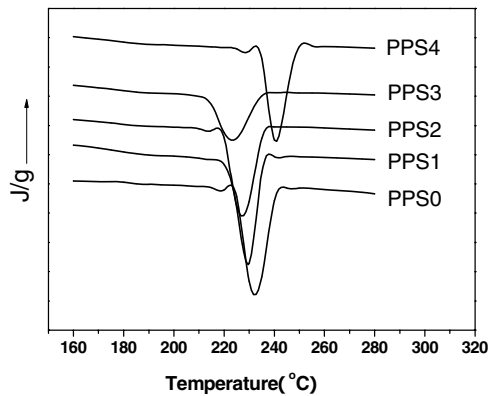

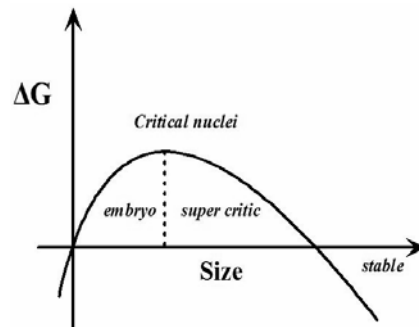Fig.2 DSC cooling curves of PPS and nanocomposites.

Fig.3 Schematic of the chemical potential difference as a function of nuclei's size during the nucleation process.

Investigation on introduction time of the nanocomposites supports the argument. In a classical nucleation and growth process the driving force for crystallization is provided by the chemical potential difference ΔG between the chemical potentials of a monomer in the amorphous and crystalline phases, respectively [18]. The nucleation step occurs at a nucleation rate, v_{nuc}, given by [18]

$$v_{nuc} \propto \exp(-E/kT) \qquad (1)$$

where E is the activation energy for nucleation. As a first approach, one may consider the induction time (t_i^{nuc}) as the period that crystallization overcomes the nucleation

barrier in order to form nucleus with critical size and the first stable nucleus to appear (Fig. 3) [19]. Therefore

$$1/t_i^{nuc} \propto \exp(-E/kT) \qquad (2)$$

Accordingly, a relative longer induction time imply comparative higher activation energy for nucleation, in another word, nucleation is prevented at the situation. Induction time can be determined by small-angle light scattering (SALS) method: the point where H_V (cross polarized) scattering appears can be taken as the onset time for crystallization, namely, the end to the induction period. Fig.3 records the H_V scattering intensity change during the crystallization process of PPS with different $CaCO_3$ filling ratio. As demonstrated in Fig. 4, it is obviously that a small amount of nanoparticles (3wt.%) prolong the induction period from 41s of the pure PPS to 49s. The result implies that the activation energy for nucleation of PPS is increased which suggest the movement of molecular chain is prevented. Whereas, a more amount of nanoparticles (10 wt.%) shorten the induction period by approximately 10s, as compared with induction period of pure PPS. This evidence suggests that the nanoparticles act as nucleating agent at the instance.
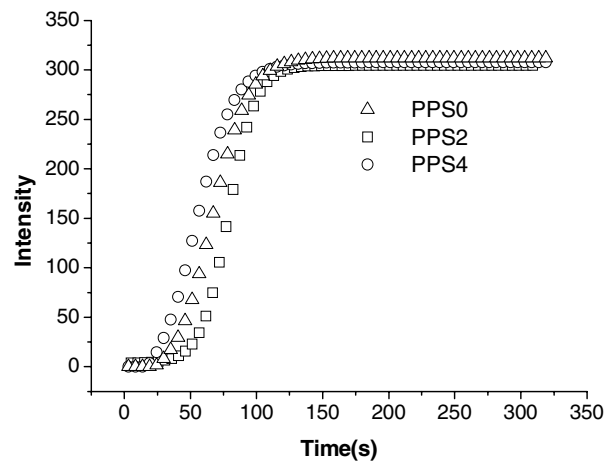

Fig.4 H_V scattering intensity change during the crystallization process of PPS and nanocomposites.

Table 2 The crystallization and melting data of the PPS and the nanocomposites (T_g: glass temperature; T_c: peak crystallization temperature determined during cooling; T_m: peak melting temperature; and X_c: wt% crystallinity of PPS (the standard heat of crystallization is taken to be 80J/g, and the crystallinity of PPS in the composites has been revised according to the content of PPS))

Sample code	T_g(°C)	T_c(°C)	X_c
PPS0	90.11	232.2	43.0
PPS1	101.56	231.5	38.9
PPS2	102.02	229.1	38.7
PPS3	99.69	227.4	38.7
PPS4	92.41	242.2	37.6

Measurement on the glass transition temperature T_g of the PPS nanocomposites gives another evidence (Table 2). As shown in Table 2, T_g of PPS is increased with the presence of $CaCO_3$ nanoparticles. Especially, T_g of PPS2 is 102.02°C, almost 11°C higher than that of pure PPS showing 90.11°C. This indicated that a small amount of dispersed nanoparticles had significant effects on the T_g of PPS. For T_g is related to the movement ability of molecular chains of polymer, so it is clear that the molecular chain of PPS is held by the even distributed nanoparticles due to great interfacial interaction, while the interaction turns weaker when nanoparticles congregating and forming particle agglomerate. In summary, $CaCO_3$ nanoparticles have two competing effects on the crystallization of PPS: inducing the nucleation but retarding the mobility of polymer chains.

Mechanical properties of the nanocomposite

The mechanical properties of the PPS/ $CaCO_3$ nanocomposites were determined by tensile strength and impact strength. The results of mechanical tests are displayed in Fig.5. The tensile strength and impact strength of the PPS nanocomposites increases with the filler content reaching a peak value of about 80MPa and 69KJ/m^2, respectively, at the filler content of 3wt.%. Compare with the pure PPS (75MPa and 23KJ/m^2), the improvement in tensile strength and in impact strength owing to the addition of the nanoparticles is about 1.07 and 3 times, respectively. In other words, we found that the addition of a small amount of nanoparticles has resulted in a slight improvement in the tensile strength and a significantly increase in the fracture toughness.
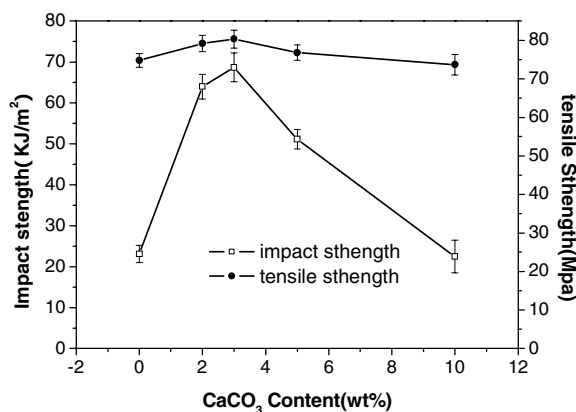

Fig.5 Impact strength and tensile strength of PPS with different filling ratio.

To analysis the tensile strength of the nanocomposites, it is commonly accepted that the strong interaction between the filler and the polymer increase the tensile strength. However, the decrease of crystallinity produces the opposite effects. A reduction in crystallinity generally reduces the tensile strength. In addition, the dispersion of the nanoparticles will have a significant effect on the strength of the nanocomposites. The dispersion is found to be better for PPS1, PPS2 and PPS3. At larger filler content in PPS4, many aggregates of nanoparticles are found. This may also accounts for the better tensile strength of the nanocomposites containing the lower wt% of filler.

Therefore, the change of tensile strength is due to the balance between the reinforcing effect and reducing crystallinity effect of the $CaCO_3$ nanoparticles.

Toughness of polymer composites is closely related to the energy-dissipating events during the crack occurring. For the particulate-filled semi-crystalline polymers, crazing, shear banding, filler-induced cavitation and the cavitation-trigged-matrix shearing have been identified as the major energy-dissipating mechanisms. It is also well accepted that whether these energy-dissipating events can happen in the specimen is determined, to a large extend, by the morphology of the semi-crystalline polymers. One of these morphological parameters is the crystal structure of the polymer, such as crystallinity. In a previous work by Ouedemi and Phillips [20], the effect of crystal structure on the toughness of polymer samples with different crystallinities was elaborated. The authors found that an increase in crystallinity would lead to lower fracture toughness.

Cavitation and cavitation-induced massive shear deformation have been identified as a dominant toughening mechanism in the rubber toughened thermoset and thermoplastic polymer blends. In a previous work, the cavitation/shear deformation was also found to be the control toughening mechanism in some rigid-rigid polymer blends [21]. In rubber-toughened polymer blend, because of the low tear strength of the rubber particles, cavitation of the rubber particle happens during cracking and it releases the high plastic constraint and enables large-scale plastic deformation in the ligament between the two cavities. In the polymer/nanoparticle composites, cavitation at the boundary of the polymer and well dispersed particles was found to have the same function as that of rubber particle cavitation [16, 22].

For our case, it is reasonable to propose that the absence of the spherulites must have a positive effect on the toughness of the nanocomposites. On the other hand, we did find massive plastic deformation on the fracture surface of the nanocomposites was accompanied by a great deal of voids, which was clearly caused by matrix cavitation due to the addition of the nanopartilces. As demonstrated by the SEM micrographs in Fig.6 (a), the fracture surface of the PPS2 has a highly plastically deformed zone filled with micron voids. The matrix between these voids are stretched and deformed extensively. The fracture surface of the PPS0 is, however, smooth and featureless (Fig.6 (b)). Base on this microscopic observation and foregoing discussion, we believe that the cavitation-induced shear deformation is most probably the dominant energy-dissipating event responsible for the very high impact strength of the nanocomposites with a small amount of particle loading. Firstly, the $CaCO_3$ nanoparticles, which reduce crystallinity of the PPS, change the morphological structure of the matrix. Secondly, the nanoparticles act as stress concentrator and promote cavitation at the particle-polymer boundaries. A previous study by Chan [16] on $CaCO_3$ nanoparticles-filled PP (4.8wt% $CaCO_3$ in PP) indicated that the $CaCO_3$ nanoparticles were dispersed inside the spherulites and there was a thin layer of amorphous PP encapsulating the $CaCO_3$ particles. Based on this proposed morphological structure, numerous cavitation sites will be created at the interface between the $CaCO_3$ particles and the amorphous layers. It is quite possible that the $CaCO_3$-filled PPS has a morphological structure similar to that of the $CaCO_3$-filled PP. According to this proposed morphological structure, a large number of cavitation sites will be created at the inter face between the nanoparticles and the amorphous layers. The formed cavities will release the plastic constraint in the matrix and trigger large-scale plastic deformation, leading to great improved fracture toughness. Although the exact micromechanical deformation mechanisms in impact are not very clear to us and still under investigation, it is

reasonable to believe that the toughening mechanism proposed for the cavitation-induced massive shear deformation is plausibly the main mechanism.
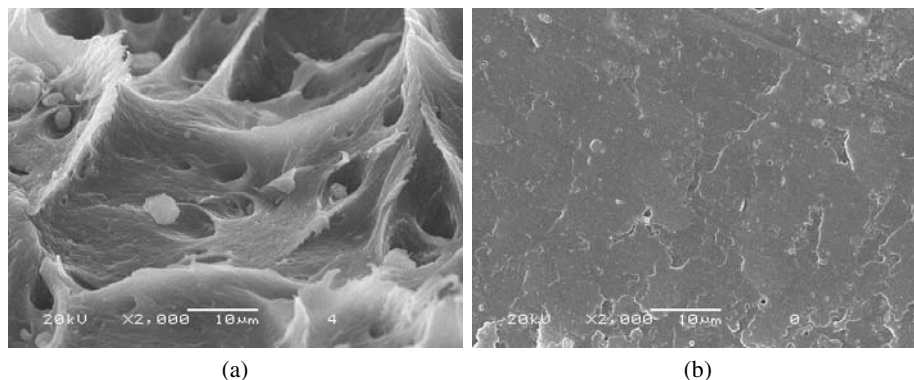

(a)   (b)

Fig.6 SEM micrographs of the impact fracture surface of the nanocomposites and PPS.

As far as the nanocomposites with a larger amount of particle loading is concerned, the nanoparticles can not be evenly distributed, and the incompact particle agglomerate can not releases the high plastic constraint and cause large-scale plastic deformation in the ligament between the two cavities. Thus, the PPS/CaCO$_3$ nanocomposites appear to be less tough with higher levels of CaCO$_3$ content.

Conclusion

PPS composites with CaCO$_3$ nanoparticles (40-60nm) were prepared. The toughness of the nanocomposites was found substantially higher than that of the pure PPS. The SPM study showed that the nanoparticles were well dispersed in the PPS matrix at low levels of CaCO$_3$ content. The evenly distributed nanoparticles had two competing effects on the crystallization of PPS: inducing the nucleation but retarding the mobility of polymer chains. A small amount of nanoparticles could also result in a slight improvement in the tensile strength and a significantly 300% increase in the fracture toughness. The cavitation-induced massive shear deformation is plausibly the main toughening mechanism. However, with an increasing loading of CaCO$_3$, the nanoparticles could not be evenly distributed and form agglomerates. The incompact particle agglomerate would lead to a decrease in both tensile and impact strength.

References

[1]   An J, Suzuki T, Ougizawa T, Inoue T, Mitamura K, Kawanishi K (2002) Journal of marcomolecular Science- Physics 41: 407
[2]   Lee S, Chun BC (1998) Polymer 39:6441
[3]   Daoust D, Bebelman S, Godard P (1996) Polymer 37:3879
[4]   Park HJ, Chun BC (1996) Polymer Bulletin, 37: 103

[5]   Zou H, Zhang Q, Tan H, Wang K, Du RN, Fu Q (2006) Polymer 47: 6
[6]   Yu L, Yang S, Liu W, Xu Q e (2000) Polymer Engineering and Science 40: 1825
[7]   Mei Z, Chung DDL (2000) Polymer and Polymer Composites 8: 319
[8]   Ramanathan T, Bismarck A, Schulz E, Subramanian K (2001) Composites Science and Technology 61:1703
[9]   Suprakas SR, Masami O (2003) Macromolecular Rapid Communications 24: 815
[10] Ottaviani MF, Valluzzi R, Balogh L (2002) Macromolecules 35: 5105
[11] Kim BH, Jung JH (2002) Macromolecules 35:1419
[12] Galgali G, Ramesh C (2001) Macromolecules, 34:852
[13] Kim GM, Lee DH, Hoffman B, Kressler J, Stőppelmann G (2000) Polymer 42: 1095
[14] Ma CG, Rong MZ, Zhang MQ, Friedrich K (2005) Polymer Engineering and Science 45: 529
[15] Yang K, Yang Q, Li GX, Sun YJ, Feng DC (2006) Materials Letters 60: 805
[16] Chan C, Wu JS, Li J, Cheung Y (2002) Polymer 43: 2981
[17] Rong M, Zhang M, Zheng Y, Zeng H, Walter R, Friedrich K (2001) Polymer 42: 167
[18] Strobl G (1996) The physics of polymer. Berlin: Springer
[19] Wunderlich B (1973) Macromolecular physics, Volume 2: Crystal Nucleation Growth, Annealing. New York: Academic Press
[20] Ouedemi M, Philips PJ (1996) Journal of Engineering and Applied Science, 2: 2312
[21] Parker DS, Sue H, Huang J, Yee AF (1990) Polymer, 31:2267
[22] Wu J, Yu D, Mai Y, Yee A. F (2000) Journal of Material Science, 35: 307